

## Geochronology and Geochemistry of Upper Proterozoic Granites from Southern Bénin

U. G. CORDANI<sup>1</sup>, K. KAWASHITA<sup>1</sup>, K. R. B. VANCINI<sup>1</sup>, A. BORIANI<sup>2</sup>,  
B. BIGIOGGERO<sup>2</sup>, P. CADOPPI<sup>3</sup> and R. SACCHI<sup>3</sup>

<sup>1</sup>Instituto de Geociências, USP, C.P. 20899, 01498 São Paulo, Brasil

<sup>2</sup>Dipartimento di Scienze della Terra, Via Botticelli, 23, 20133 Milano, Italia

<sup>3</sup>Dipartimento di Scienze della Terra, Via Accademia delle Scienze, 5, 10123 Torino, Italia

*Manuscrito recebido em 12 de maio de 1993; aceito para publicação em 27 de julho de 1993*

### ABSTRACT

The Upper Proterozoic basement of Bénin, like that of nearby Nigeria and like the "polycyclic" basement of Central Hoggar, belongs to the hinterland of the Pharusian Chain (Pan-African Trans-Saharan Belt) generated by the collision between the (passive) margin of the West African craton and the (reactivated) margin of the Tuareg Shield and its southern extension. As compared to the Adrar des Iforas region, Bénin displays a distinctive lack of an early, volcanic arc development.

Rb-Sr dating of subalkaline, meta-aluminous, syn-kinematic granite forming tabular bodies near Dassà-Zoumé and near Savé yielded two WR isochron ages of  $650 \pm 35$  Ma (I.R. = 0.7043) and  $705 \pm 70$  Ma (I.R. = 0.7045). Emplacement of these bodies was clearly controlled by transcurrent movements along the Kandi Fault System (itself a continuation of the continent-sized "4°50'" Lineament).

The analyzed granites are comparable with those of Central Hoggar and of North-Central Nigeria on the ground of field, geochronological and geochemical data; they also display some affinities with the late-tectonic granites of the Adrar des Iforas. They are expected to find their Brazilian continuation in the Chaval Granitoids west of Fortaleza, but data for comparison are inadequate.

**Key words:** Pharusian Chain, Proterozoic, geochronology, geochemistry.

### INTRODUCTION

The Upper Proterozoic basement in Bénin ("Unité de la Plaine du Bénin": refs. in Bessoles & Trompette, 1980) can, like that in nearby Nigeria, be regarded as the equivalent of the "polycyclic" basement of the Central Hoggar (see e.g. Black, 1984). This assemblage forms part (Black *et al.*, 1979) of the hinterland of the Pharusian Chain (Pan-African Trans-Saharan Belt) generated by the collision between the (passive) margin of the West African craton and the margin (reactivated over Benioff zone) of a palaeocontinent comprising the Tuareg shield and its southern extension between

Togo and Cameroon ("Dahomeyen" in the early French literature) (Fig. 1).

In Bénin, as in Central Hoggar, this basement is considered to be formed of ancient (primarily "Eburnean" = c. 2000 Ma) crust reworked during the Upper Proterozoic orogenic event (or "Pan-African" event, if we use this term in a wider sense than that originally defined by Kennedy, 1964, i.e. about 500 Ma).

The Pan-African orogeny brought about (Aa.Vv., 1989): (1) generalized radiometric rejuvenation of its minerals; (2) both brittle and ductile deformation; (3) as yet incompletely evaluated metamorphic transformations; (4) emplacement of

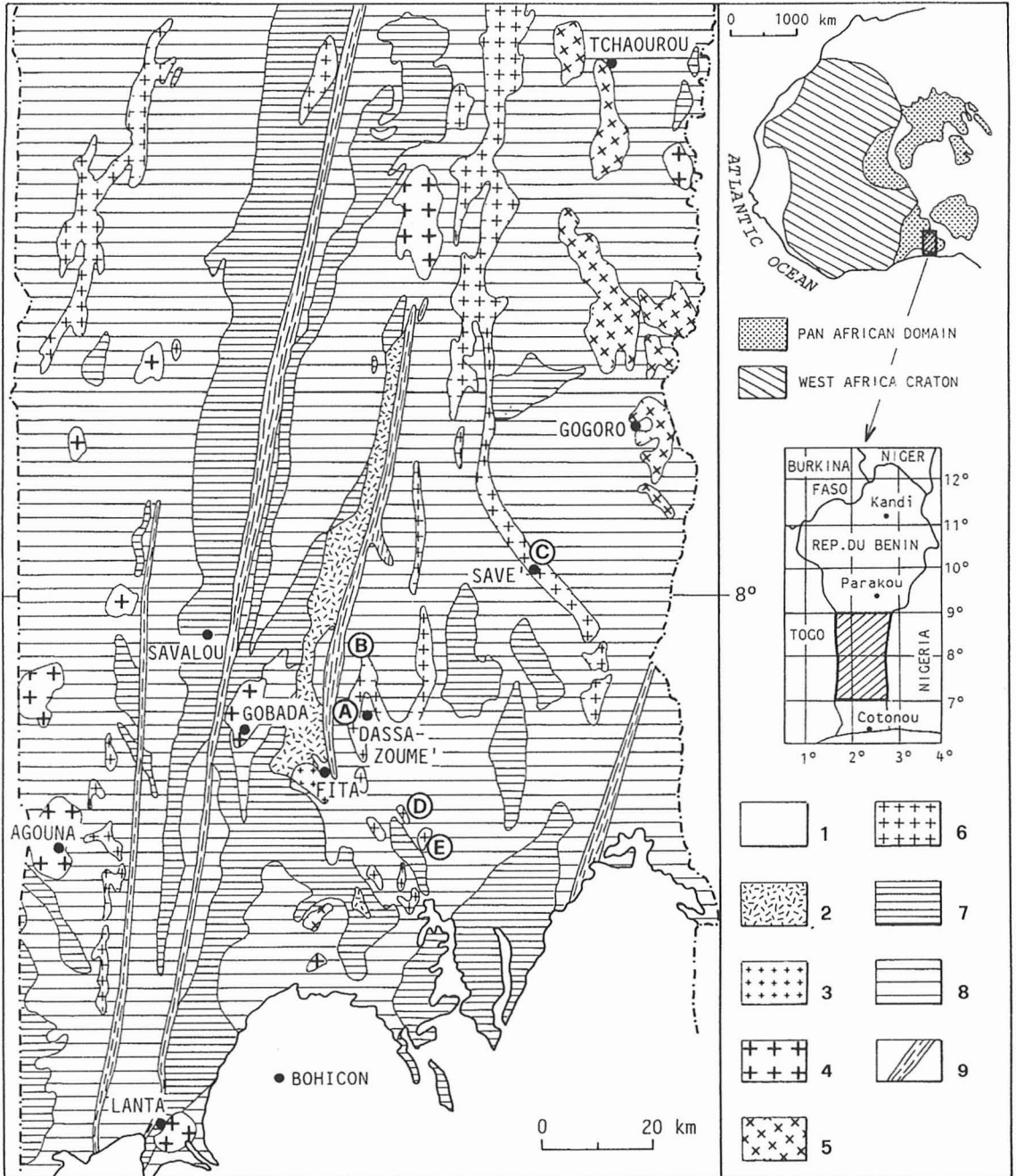


Fig. 1 — Geological sketch-map of the crystalline basement of Bénin south of the 9th parallel (mainly from Aa.Vv., 1989). (1) undifferentiated phanerozoic covers; (2) Volcano-sedimentary sequences; (3) Alkali-rich granite of Fità; (4) Equigranular granites; (5) Porphyritic granites (Gogoro-type); (6) Concordant porphyritic metagranites (Dassà-Zoumé type); (7) High-grade metamorphic basement; (8) Biotite ± amphibole gneisses, migmatites; (9) Mylonites of the Kandi Fault System. Letters A to E correspond to the locations of the described in Tab. II.

granitic rocks. These processes occurred in various phases of the orogenic event, as shown by the varying degrees of deformation and the different geometry of the units. Four types of granitoids have been distinguished on several grounds (shape of the body, texture, geochemistry) (Bigioggero *et al.*, 1988):

I) porphyritic granite with a strong planar fabric forming tabular bodies ("Dassà" meta-granite);

II) porphyritic granite with a weak or non-existent planar fabric outcropping as irregularly shaped or subcircular bodies ("Gogoro-Parokou" granite);

III) undeformed, granular granite with an isotropic fabric, rich in both microgranular and surmicaceous enclaves, and forming circumscribed bodies (Lanta, Gobada, Agouna Granites);

IV) undeformed, granular granite with an isotropic fabric and alkalic tendency, identified in a single body (Fita Granite) in association with a coeval volcano-sedimentary sequence.

Taken as a whole, field information and the admittedly very scanty geochronological results (see *infra*) show that the I to IV granite sequence approximately corresponds to the chronology of emplacement. Types (I) and (II) together correspond to the "Older Granites" of Nigeria, which have been dated at around 610 Ma (van Breemen *et al.*, 1977, Tubosum *et al.*, 1984). In Bénin, a granite with characters intermediate between type (I) and type (II) ("Granite de Savé") has been dated at about 600 Ma by Vachette (1975) on the basis of a WR-biotite Rb-Sr isochron. Type (III) is tentatively attributed to the Lower Palaeozoic (refs. in Aa.Vv., 1989).

We concentrated our attention on the synkinematic ("Dassà type") granite in order to date not only granite emplacement, but also tectonics.

Two bodies of this granite (outcropping near the villages of Savè and Dassà-Zoumé), in fact, were chosen for whole rock Rb-Sr dating. The Dassà body displays a particularly instructive large-scale folding.

It forms a tabular body with the complex geometry illustrated in the block diagram in Fig. 2. The structure consists of an eastern, open synform with a moderate, northern axial plunge and a west-

ern, more compressed antiform with a sub-vertical axis. The latter is adjacent to a fault belonging to the system of large, N-S trending transcurrent (sinistral) faults collectively known as "Faille de Kandi", itself probably the southern continuation (Guiraud & Alidou, 1981) of the fundamental "4°50'" lineament (Caby, 1968). The granite displays a planar fabric perfectly parallel to the borders and, if taken as a whole, to the structural trends of the country rock. This feature is the result of both the parallelism of the K-feldspar phenocrysts and a superposed, concordant, mylonitic fabric. There is also a N-S trending, sub-horizontal lineation conferred by elongation of the K-feldspar phenocrysts. The geometry of the body can be explained by regarding the attitude of its sub-vertical western part as primary and later modified by drag folds associated with the Kandi Fault. Other explanations, however, can not be excluded.

#### THE SPECIMENS

The specimens were taken from both the main porphyritic ("Dassà") facies and the heterogranular or slightly porphyritic facies locally associated with it in smaller bodies ("Tré" type) (Bigioggero *et al.*, 1988). They include a few mafic and acidic dikes (see later). In the field, the Tré facies displays clear evidence of intrusion (by a probable magmatic stoping mechanism) into the Dassà-type granite. Even so, the chemical, mineralogical and textural characters of the two lithotypes are identical, and a cogenetic nature may thus be assumed. Their composition (as described by Bigioggero *et al.*, 1988) ranges from granodiorite to monzogranite. The microcline-perthite megacrysts (where present) include idiomorphic plagioclase and/or biotite, and are immersed in a matrix formed of polygonized plagioclase and myrmekite. The biotite is recrystallized, as shown by its decussate structure. The plagioclase has an An concentration of about 30%. The accessory minerals are very abundant: mainly sphene and an epidote with a metamictic core, together with apatite, ilmenite, leucoxene, zircon and fluorite. In the Dassà type, there are numerous dark xenoliths, in

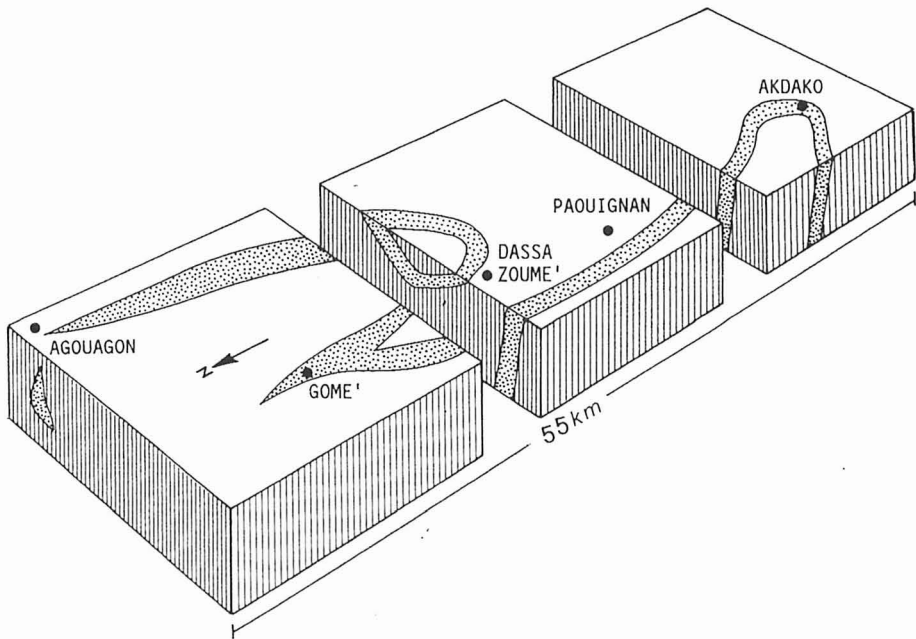


Fig. 2 — Idealized structure of the magmatic body of Dassà-Zoumé (stippled); see text for description.

which boudinaged, syn-granitic basic dykes can often be recognized.

The fabric suggests that a subsolidus deformation (mylonitic fabric) has overprinted a previous orientated fabric that developed under late-magmatic conditions (cf. the parallelism of the undeformed phenocrysts both with each other and with the borders of the granite body, as well as the ubiquitous nature of the parallel fabric compared with the heterogeneous and discontinuous nature of a tectonic fabric; see also Paterson *et al.* (1989)).

Thirteen specimens from the five localities shown in Fig. 1 were analysed. Sample locations and the main petrographic features are reported in Tab. I.

**GEOCHEMISTRY**

The rocks analyzed (Tab. II) form a subalkaline series with high K<sub>2</sub>O content and with SiO<sub>2</sub> values ranging from 61 to 74% (Fig. 3). In the R<sub>1</sub>R<sub>2</sub> diagram (de La Roche *et al.*, 1980; Fig. 4a), the samples cover a range of composition from tonalites to granites. In the A/B diagram of Fig. 4b (Debon & Le Fort, 1988), the samples form a metaluminous “Cafemic” series. The ORG normal-

ized spidergrams (Harris *et al.*, 1986) show enrichment in LILE + Th and a moderate Nb anomaly, together with very limited HFSE and HREE depletion (Fig. 5a). The REE patterns (Fig. 5b) display pronounced fractionation and a LREE/HREE ratio of about 30. The negative Eu anomaly is always very distinct (Eu/Eu\* about 0.5).

This geochemistry is substantially similar to that of granitoid series from an “orogenic” (*sensu*

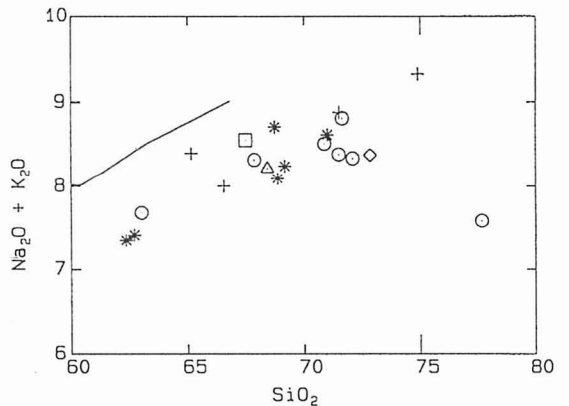


Fig. 3 — Total alkalis/silica diagram for the granitoid rocks of the Dassà-type. Symbols refer to the sampling localities (Fig. 1 and Tab. I and II): A — cross; B — square; C — asterisk; D — triangle; E — diamond. Small circles: analyses of the Dassà-type granitoids from Bigoggero *et al.*, 1988.

**TABLE I**  
**Sample description**

Sample no.	Location in fig. 1	Co-ordinate		Sample description
		lat. (N)	long. (E)	
BE72B	(A) Dassà-Zoumé	7°50'30"	2°12'00"	Porphyritic granite with a mylonitic fabric that overprints the original magmatic texture. Metamorphic foliation mainly determined by the orientation of biotite flakes, ribbon quartz and K-feldspar porphyroclasts. Perthitic K-feldspar, mildly zoned plagioclase (partly altered to sericite and carbonate), quartz and biotite are the main magmatic components. Accessories: sphene, opaque minerals, metamictic allanite, apatite, zircon, fluorite. Muscovite, carbonate and epidote are secondary phases.
BE74B,C	(A) Dassà-Zoumé	7°50'30"	2°12'00"	Porphyritic granodiorite with marked mylonitic fabric. Metamorphic foliation mainly due to the orientation of biotite. Zoned plagioclase (partly recrystallized into fine-grained aggregate), K-feldspar (now microcline), quartz, biotite (recrystallized) and green hornblende (rare, partly gone into biotite) are the main magmatic phases. Accessories as in sample BE72B except fluorite.
BE75	(A) Dassà-Zoumé	7°50'30"	2°12'00"	Aplitic dike with granular fabric. It shows partial metamorphic recrystallization into fine-grained aggregate. K-feldspar, plagioclase and quartz are the main phases. Biotite (totally recrystallized), muscovite with myrmekitic texture, epidote and accessories (opaque minerals, sphene, zircon and apatite) are < 5%.
BE134A	(C) Savé	8°02'30"	2°30'00"	Granite dike with granular fabric. Partial metamorphic recrystallization of all components. Crude foliation defined by orientation of biotite flakes. Mildly zoned plagioclase, perthitic K-feldspar, quartz, biotite and (rare) green hornblende are the main components. Accessories as in sample BE72B except fluorite.
BE138A,B	(C) Savé	8°02'30"	2°30'00"	Tonalitic dike with granular fabric. A marked metamorphic foliation is due to the orientation of biotite flakes. Zoned plagioclase (partly altered to sericite), quartz, biotite and subordinate K-feldspar are the main phases. Accessories: sphene, metamictic allanite, apatite, zircon and opaque minerals included in sphene. Secondary carbonate.
BE139A,B,C	(C) Savé	8°02'30"	2°30'00"	Porphyritic granodiorite. Crude metamorphic foliation defined by parallel flakes of biotite concentrated in thin leaves. Mildly zoned plagioclase (partly altered to sericite and recrystallized), K-feldspar (large porphyroclasts of microcline), quartz and biotite as main phases. Accessories as in sample BE138A,B.
BE150C	(B) Gomé	7°53'00"	2°12'30"	Porphyritic granodiorite with strong mylonitic fabric. K-feldspar and plagioclase porphyroclasts surrounded by aggregate. Metamorphic foliation mainly defined by orientation of porphyroclasts and of biotite. Magmatic components as in sample BE74B,C with more epidote.
BE154	(E) Assiyo	7°34'30"	2°17'30"	Porphyritic granite with strong mylonitic fabric. All the magmatic components are recrystallized in fine-grained aggregate except for a few perthitic K-feldspar (now microcline) and plagioclase (altered to sericite) porphyroclasts. Accessories: mainly metamictic allanite (rimmed by epidote) and rare sphene, apatite and zircon.
BE155	(D) Lissa	7°42'00"	2°16'00"	Porphyritic granodiorite similar to sample BE139A,B,C. Metamorphic foliation defined by orientation of K-feldspar porphyroclasts and biotite flakes. Secondary muscovite.

TABLE II  
Geochemical data

Sample	BE72B	BE74B	BE74C	BE75	BE134A	BE138A	BE138B	BE139A	BE139B	BE139C	BE150C	BE154	BE155
SiO <sub>2</sub>	70.93	66.37	64.39	74.43	70.30	61.62	61.96	68.15	67.56	68.49	67.22	72.18	67.72
TiO <sub>2</sub>	0.48	0.89	0.88	0.03	0.56	1.56	1.50	0.56	0.70	0.66	0.81	0.30	0.81
Al <sub>2</sub> O <sub>3</sub>	13.73	14.98	15.43	13.71	13.53	14.73	14.88	15.42	14.44	14.41	14.16	13.64	14.14
Fe <sub>2</sub> O <sub>3</sub>	2.82	5.01	5.08	0.65	3.83	8.03	7.33	3.22	4.08	4.01	5.54	2.57	4.65
MnO	0.03	0.07	0.07	0.01	0.03	0.10	0.08	0.02	0.05	0.04	0.07	0.03	0.04
MgO	0.46	1.29	1.33	0.01	0.55	1.67	1.62	0.70	0.91	0.88	0.77	0.32	0.73
CaO	1.77	3.13	3.22	1.26	1.67	3.84	3.77	2.41	2.41	2.27	2.40	1.56	2.37
Na <sub>2</sub> O	2.87	3.40	3.37	3.11	2.42	3.00	3.16	3.27	3.04	2.87	2.70	3.06	2.75
K <sub>2</sub> O	5.94	4.58	4.94	6.16	6.12	4.26	4.16	5.37	4.90	5.30	5.83	5.25	5.39
P <sub>2</sub> O <sub>5</sub>	0.17	0.01	0.12	0.01	0.01	0.01	0.34	0.01	0.01	0.07	0.10	0.19	0.36
LOI	0.47	0.59	0.49	0.33	0.65	0.90	0.80	0.51	0.54	0.62	0.61	0.63	0.64
Total	99.67	100.32	99.32	99.71	99.67	99.72	99.60	99.64	98.64	99.62	100.21	99.73	99.60
Ba	856	1332	1459	107	1037	1188	1152	1262	1071	1186	1184	562	1124
Be	2.9	2.7	3.0	3.2	1.2	2.6	2.5	2.2	2.2	2.0	2.1	3.7	2.2
Co	17	12	15	32	23	20	28	19	13	12	23	12	6
Cr	12	38	33	23	12	25	23	17	23	26	21	7	9
Nb	44	37	34	64	25	33	31	21	22	14	58	26	35
Ni	10	19	25	5	9	15	15	16	20	7	7	6	9
Rb	254	196	177	171	226	218	208	207	215	220	201	242	212
Sr	197	326	358	51	227	330	342	300	266	266	246	145	246
Th	42.56	20.76	19.16	17.64	56.63	21.94	37.24	29.16	38.78	36.02	32.40	33.84	35.79
U	4.88	2.34	1.87	8.37	1.55	1.59	22.91	2.23	1.84	2.01	1.71	3.15	2.67
V	18	71	71	5	25	63	62	28	32	30	27	9	25
Y	71.89	44.61	44.90	44.18	38.12	37.77	40.43	21.39	26.45	23.88	52.65	26.25	35.55
Zn	66	83	96	10	76	121	111	72	89	89	105	73	93
Zr	370	464	452	72	494	723	540	303	408	443	580	232	469
La	112.63	118.67	118.80	1.97	216.32	91.37	106.21	90.98	114.14	101.54	150.81	63.15	120.69
Ce	219.38	224.65	214.48	9.82	401.40	198.05	221.48	186.12	232.79	198.26	227.27	133.76	236.49
Nd	91.90	88.03	85.33	3.14	155.35	87.32	98.19	73.91	91.79	83.50	122.34	57.24	103.39
Sm	17.54	14.84	14.44	2.80	23.46	14.81	16.47	11.79	14.67	13.28	20.23	10.60	17.20
Eu	1.90	2.40	2.24	0.28	2.12	2.21	2.45	1.74	1.99	1.83	2.63	1.17	2.13
Gd	14.79	11.51	11.07	5.25	15.32	11.11	11.68	7.92	9.45	9.03	15.23	8.04	12.38
Dy	12.09	7.87	7.68	8.27	7.82	7.22	7.54	4.40	5.37	4.90	10.04	5.16	7.22
Er	5.81	3.77	3.70	4.44	3.39	3.25	3.47	1.88	2.28	2.11	4.48	2.15	2.91
Yb	4.87	3.18	3.14	3.85	2.55	2.48	2.64	1.35	1.72	1.57	3.32	1.67	2.13
Lu	0.83	0.56	0.57	0.65	0.45	0.48	0.48	0.24	0.31	0.29	0.58	0.31	0.37
Y + Nb	115.39	81.61	78.90	108.18	63.12	70.77	71.43	42.39	48.45	37.88	100.62	52.25	70.55
Rb/Sr	1.29	0.60	0.49	3.35	1.00	0.66	0.61	0.69	0.81	0.83	0.82	1.67	0.86

*lato*) environment (Harris *et al.*, 1986), in which the LILE, Th and LREE enrichments are evidence of the influence of a crustal component.

The involvement of upper crust rocks in the genesis of these intrusives is ruled out by their metaluminous character and other geochemical features like the low Rb/Sr ratio.

The Dassà complex displays a relatively broad range of compositions and the constant presence of a negative Eu anomaly: fractional crystallization processes are suggested to have played an

important role. As far as major phases are concerned, negative Rb vs. Sr and Rb vs. Ba correlation (Fig. 6a and 6b) could suggest that the fractionating assemblage is dominated by feldspars + Amph ± Bt in trend 1 followed by prevailing K-feldspar + Bt removal in trend 2, in which Rb correlates positively with Sr and Ba. Some post-tectonic Pan-African granites from Bénin (Bigioggero *et al.*, 1988) show a significantly different composition and a lower Sr enrichment. A comparison can also be made with the late-tectonic

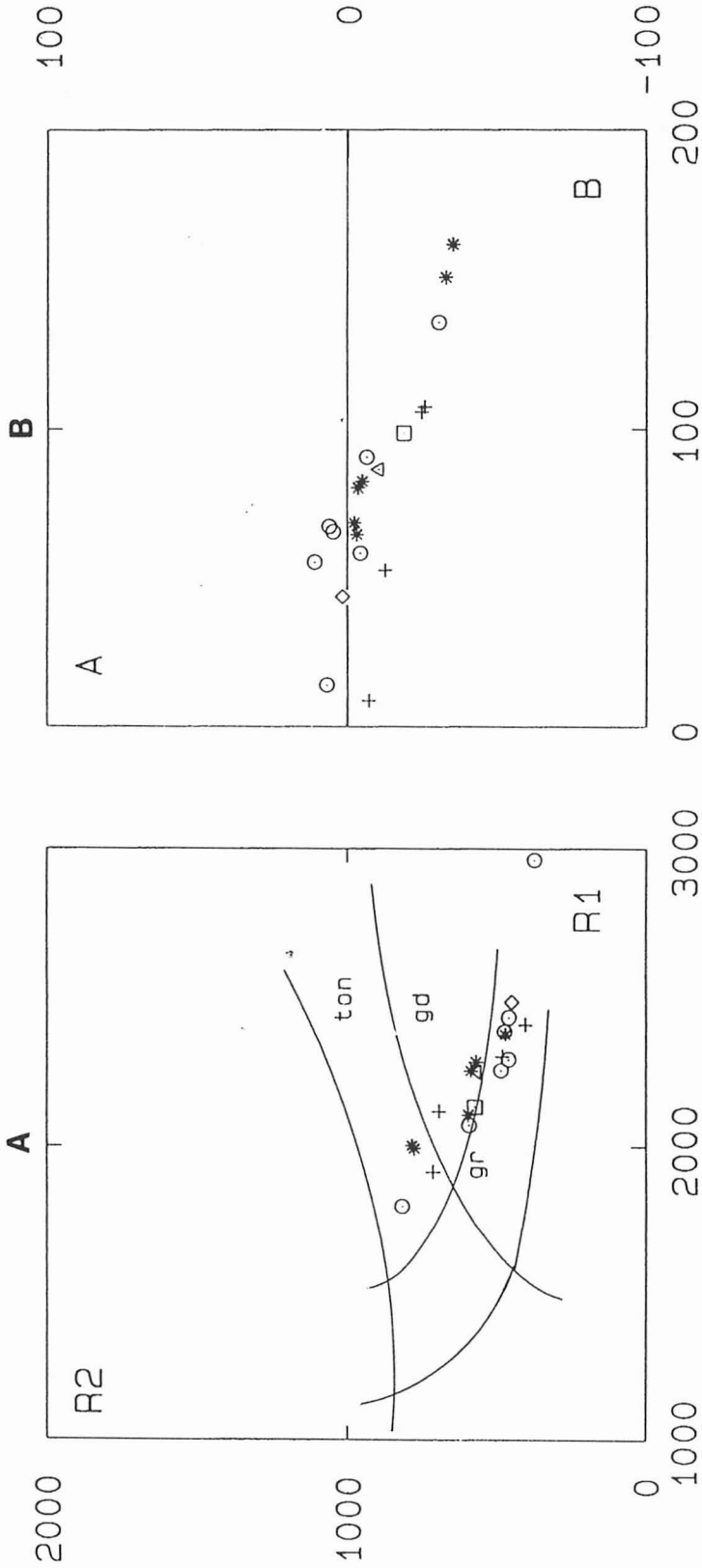


Fig. 4 — a) R1R2 classificative diagram (La Roche *et al.*, 1980), symbols as in Fig. 3; ton = tonalite; gd = granodiorite; gr = granite. b) A (alumina saturation index) vs. B (mafic phases content) diagram, from Debon & Le Fort (1988).

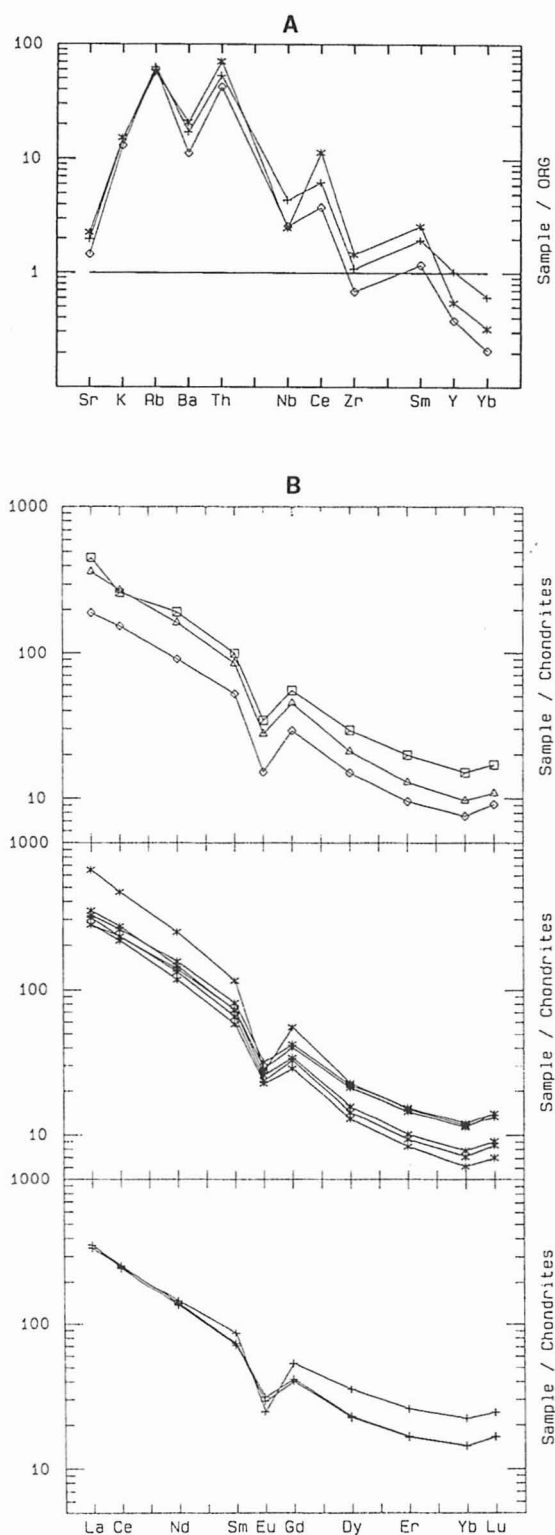


Fig. 5 — Normalized spidergrams for the analysed samples; symbols as in Fig. 3. a) samples of “granitic” composition normalized to the ORG (Ocean Ridge Granites) values of Harris *et al.*, (1986). b) Chondrite normalized REE patterns.

and post-tectonic suites of the Adrar des Iforas (Liégeois & Black, 1984). Here, too, there is a geochemical difference of the same type, namely significantly higher Sr enrichment in the older, “tardi-tectonique” suites.

## GEOCHRONOLOGY

The age determinations were obtained at the Geochronology Research Center of the University of São Paulo and the analytical data are reported in Tables III and IV. The first one reports the results obtained in three biotites by the K-Ar method, and the second shows the complete Rb-Sr determinations. The methods have been described elsewhere, e.g. in Cordani & Iyer (1979). The analytical work was done in November-December 1987. At that time, the analytical precision for the K-Ar method was within a few per cent of the indicated age values, and the individual experimental errors (at  $2\sigma$  level) are indicated in Table III. Rubidium and strontium determinations are by X-ray fluorescence, with individual precision of the measurements of about 2%; on the other hand, however, the precision in the Rb/Sr ratio is better, usually below 1%. The  $^{87}\text{Sr}/^{86}\text{Sr}$  ratios were measured on unspiked samples, with an overall precision better than 0.01%. Accuracy can be evaluated from thirteen analyses of the interlaboratory standard NBS-987, run concurrently in the same instrument (a VG-354 solid source mass spectrometer), with an average value of  $0.71025 \pm 0.00003$ . Regression analyses of the Rb-Sr isotopic data were carried out using the method of Williamson (1968), and the decay constants employed were those from Steiger & Jäger (1977).

Three samples from the same outcrop (BE72B, BE74B and BE74C from locality A in Fig. 1) near Dassà-Zoumé, representing the main porphyritic Dassà-type, yielded a Rb-Sr whole-rock isochron age of  $650 \pm 35$  Ma (MSWD = 1.084), with  $^{87}\text{Sr}/^{86}\text{Sr}$  initial ratio of  $0.7043 \pm 0.0009$  (Fig. 7a). The age value is interpreted as the crystallization of the granitic body.

In the same Fig. 7a, for visual comparison only, the analytical point of sample BE75 was included. It belongs to an aplite dike from the same

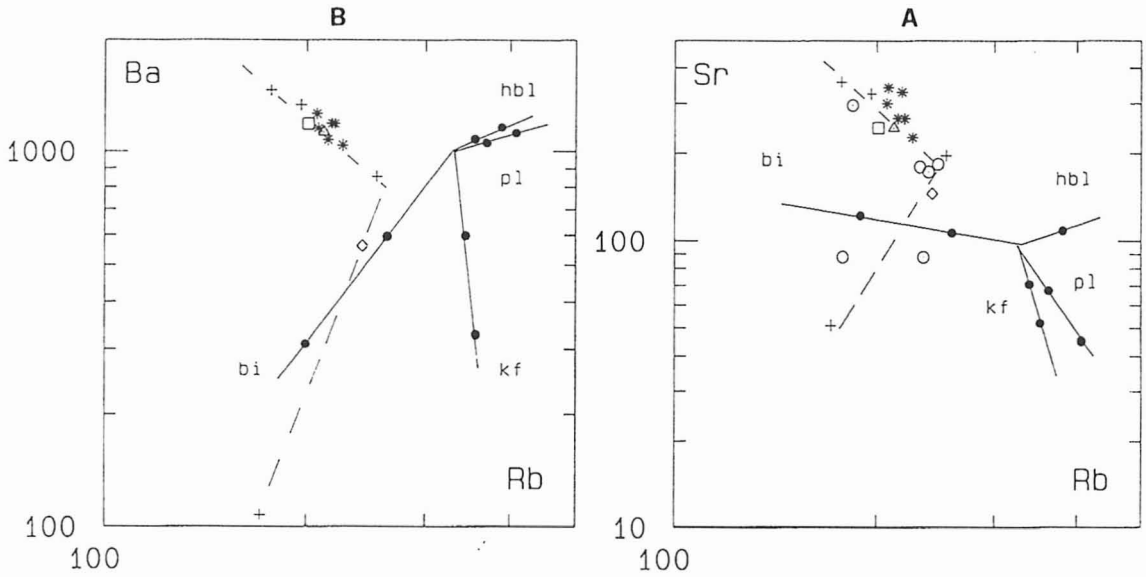


Fig. 6a and b — Rb/Sr and Rb/Ba log/log plots. Crystal fractionation trends 1 and 2 can be referred to feldspar + amphibole ± biotite removal and K-feldspar + biotite removal. Thick marks on fractionation vectors indicate 10% steps. Kf = K-feldspar; Pl = plagioclase; Bi = biotite; Hbl = amphibole; Cpx = clinopyroxene.

TABLE III  
K-Ar results on biotites

Sample	Location	Rock type	Lab n°	%K	<sup>40</sup> Ar rad (x10 <sup>-6</sup> ccSTP/g)	% <sup>40</sup> Ar atm	Age (Ma)
BE138B	(C) Savé	tonalitic dike	6150	7.673	173.5	2.58	505 ± 12
BE150A	(B) Gomé	porphyritic granodiorite	6152	4.968	119.6	0.98	533 ± 14
BE155	(D) Lissa	porphyritic granodiorite	6153	7.163	166.4	8.56	516 ± 12

TABLE IV  
Rb-Sr analytical data

Sample	Location	Rock type	Material	Lab n°	Rb, ppm	Sr, ppm	<sup>87</sup> Rb/ <sup>86</sup> Sr	<sup>87</sup> Sr/ <sup>86</sup> Sr	Calc. age (Ma) <sup>§</sup>
BE72B	(A) Dassà-Zoumé	porphyritic granite	Whole rock	8995	248.6	206.0	3.503	0.7366	632 ± 44
BE74B	(A) Dassà-Zoumé	porphyritic granodiorite	Whole rock	8986	193.8	335.2	1.765	0.7202	—
BE74C	(A) Dassà-Zoumé	porphyritic granodiorite	Whole rock	8987	186.4	363.6	1.485	0.7178	—
BE75	(A) Dassà-Zoumé	aplitic dike	Whole rock	8988	171.7	51.1	9.799	0.7856	577 ± 21
			Feldspar	9040	163.2	40.7	11.716	0.7965	548 ± 18
BE134A	(C) Savé	granitic dike	Whole rock	8989	205.9	229.3	2.604	0.7290	645 ± 56
BE138A	(C) Savé	tonalitic dike	Whole rock	8990	212.6	333.2	1.850	0.7236	—
BE138B	(C) Savé	tonalitic dike	Whole rock	8991	203.5	354.6	1.663	0.7210	—
BE139A	(C) Savé	porphyritic granodiorite	Whole rock	8992	199.8	304.6	1.901	0.7237	—
			Feldspar	9041	80.9	248.1	0.945	0.7194	—
BE139B	(C) Savé	porphyritic granodiorite	Whole rock	8993	208.7	273.6	2.212	0.7269	694 ± 66
BE139C	(C) Savé	porphyritic granodiorite	Whole rock	8994	223.6	272.2	2.382	0.7281	680 ± 62
BE150C	(B) Gomé	porphyritic granodiorite	Whole rock	8995	186.4	245.2	2.204	0.7258	663 ± 66
BE154	(E) Assiyo	porphyritic granite	Whole rock	8996	235.6	156.2	4.381	0.7433	612 ± 36
BE155	(D) Lissa	porphyritic granodiorite	Whole rock	8997	192.6	248.2	2.250	0.7272	691 ± 65
			Feldspar	9057	90.6	221.6	1.185	0.7187	—

§ (<sup>87</sup>Sr/<sup>86</sup>Sr)<sub>0</sub> = 0.705 and <sup>87</sup>Rb = 1.42 × 10<sup>-11</sup> year<sup>-1</sup>

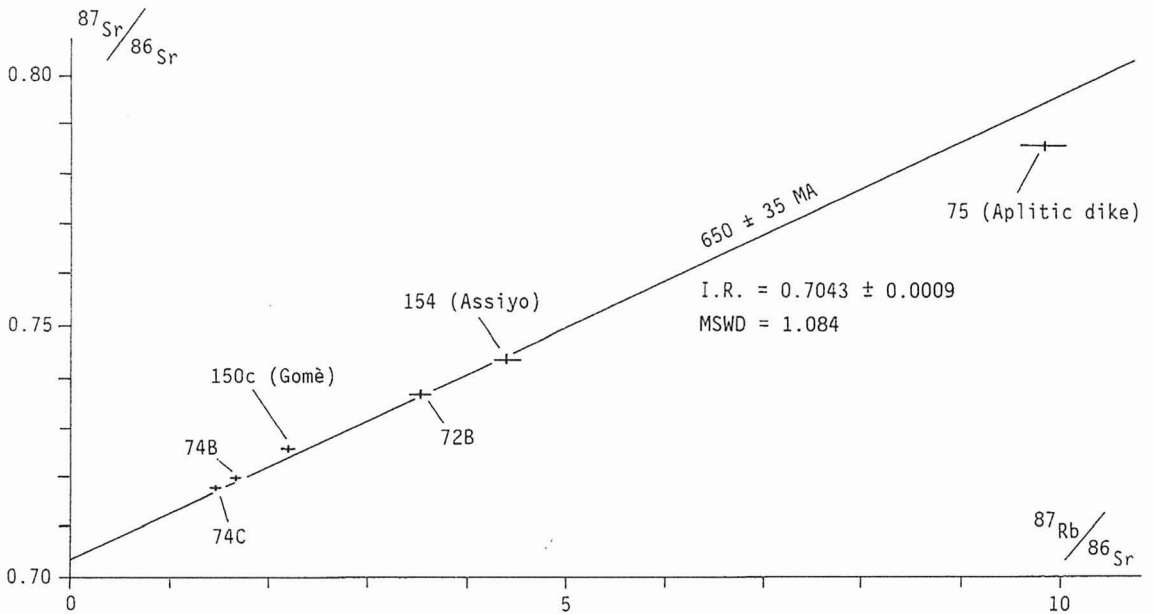


Fig. 7a — Rb and Sr isotope ratios for the different groups of samples; see text for description. Rb/Sr isochron for group A (Dassà-Zoumé) samples. Samples BE 75, BE 150c and BE 154 were not included in the regression calculations.

outcrop, which is clearly younger than the main granite, and yielded an apparent age of about 580 Ma, when calculated with  $(^{87}\text{Sr}/^{86}\text{Sr}) = 0.705$  (see Table IV).

The analytical points of samples BE150C (from Gomé, locality B in Fig. 1) and BE154 (from Assiyo, locality E in Fig. 1) were also included in Fig. 7a, although they were not considered for the regression calculation. The position of the analytical points close to the isochron, as well

as lithological similarity, indicate a possible cogeneticity of the Dassà, Gomé and Assiyo bodies.

Fig. 7b reports the analytical points of samples from a granitic body near the village of Savé (locality C in Fig. 1), the same one already dated by Vachette (1975) on the basis of WR-biotite isochron. The Savé granite is similar to the porphyritic Dassà type, but with a less pronounced planar fabric. The analytical points of five samples corresponding to two outcrops located nearby

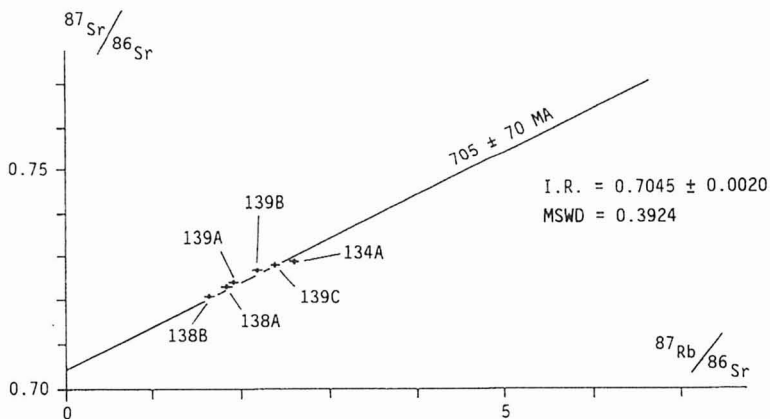


Fig. 7b — Rb and Sr isotope ratios for the different groups of samples; see text for description. Rb/Sr isochron for group C (Savé) samples. Sample BE 134A was not included in the regression calculations.

(BE138A, BE138B, BE139A, BE139B and BE139C) are reasonably aligned in the diagram of Fig. 7b, and the best fit line corresponds to an age of  $705 \pm 70$  Ma (MSWD = 0.3924) with I.R. =  $0.7045 \pm 0.0020$ . This age value appears older than the Dassà-Zoumé isochron but, because of the large uncertainty due to the restricted spread of the  $^{87}\text{Rb}/^{86}\text{Sr}$  values, as well as the relative scatter of the points in relation to the best fit line, both values may be considered concordant, within the indicated experimental errors. In the same diagram, the analytical point of samples BE134A, from a younger granitic dike, was included. It plotted below the isochron, and its calculated age is around 645 Ma (see Table IV).

A sample of granitoid collected near the village of Lissa (BE155, cf. Table IV), and belonging to the Tré type, with small feldspar phenocrysts, yielded an analytical point located practically on the best fit line for the Savé samples (see Fig. 7c). The bulk of the above data suggest that the Dassà and Tré types were formed from the same mantle source, in a relatively short period of time, somewhere between 650 and 700 Ma.

The ( $^{87}\text{Sr}/^{86}\text{Sr}$ ) initial ratios of both isochrons at Dassà and Savé are around 0.7045, a value which is too low to be associated with anatexis, or extensive crustal reworking, in agreement with the geochemical results. On the other hand, although the values are slightly high to be from a pure mantle source, they strongly suggest the principal component of the granitoid magma to be mantellic, with some degree of crustal contamination.

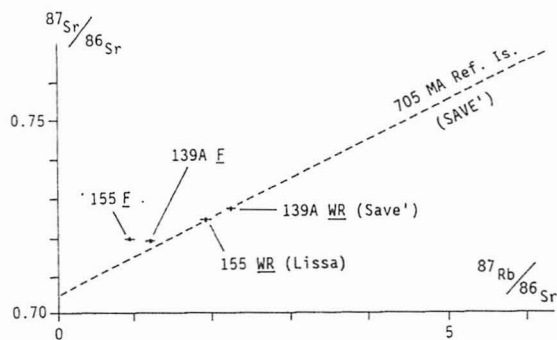


Fig. 7c — Rb and Sr isotope ratios for the different groups of samples; see text for description. Rb and Sr isotope ratios for whole rocks (WR) and isolated feldspar (F).

Some additional comments can be made taking into account the samples collected and analyzed by Vachette (1975). Of the two specimens of the Savé granite, collected in separate outcrops, one (AP 21/2), if plotted in Fig. 7a, would locate very close to the best fit line of 705 Ma, while the other would place significantly above it. In addition, taking the analytical data of the four samples of undeformed or slightly deformed granites of Sinedé and Fita (Vachette, 1975), and recalculating the apparent ages with  $\lambda_{\text{Rb}} = 1.42 \times 10^{-11}$  years<sup>-1</sup> and  $R_0 = 0.705$ , all results will cluster around 610-630 Ma. Since all samples exhibit high Rb/Sr ratios, we consider this age value as possibly significant: a late to post-tectonic episode.

Since many of the studied rocks are composed of large feldspar megacrysts included in a granitic matrix, in three cases (samples BE75, BE139A and BE155) the large crystals were separated and analysed in order to test their possible isotopic equilibrium. In the case of sample BE75, with high Rb/Sr ratio, the separated feldspar indicated a younger apparent age (see Table IV), compatible with a process of isotopic homogenization finishing at about 540-550 Ma. This apparent age value is typical of a main post-tectonic phase of the Pan-African orogeny.

In the cases of samples BE139A and BE155, the separated feldspars contain less or much less Rb than the respective whole rock (see Table IV), and their analytical points fall well above the Savé reference isochron in Fig. 8. In our opinion, this indicates chemical mobility of Rb and/or Sr among the mineral phases, in the solid state, after crystallization and emplacement. However, a complete Sr isotopic homogenization was not achieved, since the feldspar - whole rock segments do not characterize parallel mineral isochrons. The time of the final cooling of the systems may be indicated by the K-Ar biotite results in Table III, at about 510-530 Ma, when the temperature fell below 200°-250°, probably corresponding to the final event of regional uplift of the Pan-African orogeny.

## CONCLUSIONS AND REGIONAL SETTING

Let us now see how our new dating fits into a sufficiently extensive regional context comprising Nigeria, Central Hoggar, and Adras des Iforas. The foliated "syn-tectonic" and poorly foliated "late-tectonic" granites distinguished by McCurry (1973) in North-Central Nigeria are comparable with our Dassà and Gogoro-Parakou types. These granites appear to have been emplaced earlier than the one we studied in the Bénin, namely at about 610 Ma (van Breemen *et al.*, 1977), as shown by both the U-Pb concordant zircon ages and the W.R. isochrons (range of Sr initial ratios: 0.7065-0.7125).

Within the polycyclic Central Hoggar province, granitoids in the same age range as our "Dassà-type" mainly occur in the Téfedest-Atakor domain. The best isochron age for a syntectonic granodiorite is  $670 \pm 53$ , whereas post-tectonic granites yielded ages of  $550 \pm 7$  and  $514 \pm 8$  (Valette & Vitel, 1979; recalculated by Cahen & Snelling, 1984), Sr initial ratio being in the range 0.708-0.710.

The evolution of the Pharusian Chain in the Adrar des Iforas differs from that of the southern segment owing to the presence of an island-arc type pre-collisional development, with production of juvenile crust, that began > 700 Ma ago (Caby *et al.*, 1986).

As Black (1984) points out, evidence of a Cordilleran-type development is only found in an embayment (Gourma) of the margin of the West African craton, whereas, at the latitude of Bénin, the crust of the Tuareg Shield is directly thrust over the other continental margin. Post-collisional magmatism comparable with that in Bénin, though younger, was envisaged by Liégeois & Black (1984). Their late-tectonic "phase 2" includes high-K calc-alkaline porphyritic granites associated with a microgranular facies (Aoukenek adamellite), whose emplacement is regarded as having occurred only slightly later, and is dated at  $591 \pm 18$  Ma (a slightly earlier date - 615 Ma - is provided by the zircons according to Ducrot *et al.*, 1979, quoted by Boullier *et al.*, 1986). The suggested source is a depleted Upper Mantle modified

by fluids from subducted oceanic crust (see also Boullier *et al.*, 1986). On the other hand, their Sr initial ratio (0.7035) is lower than that for Dassà granites in Bénin, whereas the lithology and fabric display similar characters. In addition, there is a tectonic association with an approximately N-S lineament. A genetic link between the Pan-African granites in the 650-550 Ma range and large rhegmatic faults with a strong transcurrent movement is a general feature of the Pharusian Chain, as shown by Vitel (1975). In Mali, ages within the same range as those of Liégeois and Black have been obtained on "synorogenic granitoids" with the U-Pb method on zircons by Caby *et al.* (1985).

In conclusion, our granites display various affinities with the analogous types in the Adrar des Iforas, which have a more marked mantle character, as indicated by their lower Sr initial ratio, as well as with those of Nigeria and Central Hoggar, whose Sr initial ratios are higher. They also share with the late-tectonic granites of the Iforas a type of emplacement determined by transcurrent movements along N-S trending lineaments, together with certain geochemical affinities, as described above. The ages of comparable, syn- to late-kinematic granites from Bénin, Nigeria, Adrar des Iforas and Central Hoggar are spread over 50 to 100 Ma; no explanation is offered for the time difference, though an oblique ("docking") collision is probably involved.

If an attempt is made to compare the Bénin granitoids with those occurring in NE Brazil, in a pre-rift reconstruction, some correlation can be envisaged. The Itaporanga Granite (McMurry *et al.*, 1987) seems to be similar in age and in petrological and geochemical character; however, its type locality corresponds to a more internal domain in the orogenic belt. Another possibility could be the Chaval Granite (Brasil, 1981) which occurs west of Fortaleza, in a position more adequate to correlate with the Dassà meta-granites. However, some preliminary results by Nogueira Neto *et al.* (1989) indicate important geochemical differences and a younger Rb-Sr isochron age of about  $510 \pm 27$  Ma for the Chaval granitoids.

## ACKNOWLEDGEMENTS

B. Bigoggero and R. Sacchi gratefully acknowledge funding by the Ministry of Education (MPI "40%" grant). The work by K.R.B. Vancini was supported by The State of São Paulo Foundation for Research Support (FAPESP - Proc. 88/0274-0).

## REFERENCES

- AA.VV., (1989), Carte Géologique du socle du Bénin au Sud du 9ème parallèle à l'échelle 1:200.000. *Istituto Ricerche Breda Divisione Geomineraria, tirage provisoire inédit.*
- BESSELES, B. & TROMPETTE, R., (1980), Géologie de l'Afrique. La chaîne panafricaine "zone mobile d'Afrique centrale (partie sud) et zone mobile soudanaise". *B.R.G.M., Mém.*, **92**: 396 p.
- BIGOGGERO, B.; BORIANI, A.; CADOPPI, P.; SACCHI, R.; VEDOGBETON, N. & YEVIDE, H., (1988), Données préliminaires sur les granites du Bénin Meridional. *Rend. Soc. It. Min. Petr.*, **43**: 477-484.
- BLACK, R., (1984), The Pan-African event in the geological framework of Africa. *Pangea*, **2**: 7-16.
- BLACK, R.; BA, H.; BALL, E.; BELTRAND, J. M.; BOULLIER, A. M.; CABY, R.; DAVISON, I.; FABRE, J.; LEBLANC, M. & WRIGHT, L. I., (1979), Outline of the Pan-African Geology of Adrar des Iforas (Republic of Mali). *Geol. Rundschau*, **68**: 543-564.
- BOULLIER, A. M.; LIÉGEAIS, J. P.; BLACK, R.; FABRE, J.; SAUVAGE, M. & BERTRAND, J. M., (1986), Late Pan-African tectonics marking the transition from subduction-related calc-alkaline magmatism to within-plate alkaline granitoids (Adrar des Iforas, Mali). *Tectonophysics*, **132**: 233-246.
- BRASIL - MIN. MINAS ENERGIA/ PROJETO RADAMBRASIL, (1981), *Folha SA-24 Fortaleza: Geologia, geomorfologia, pedologia, vegetação e uso potencial da terra.* Rio de Janeiro: 488 p.
- CABY, R., (1968), Une zone de décrochement à l'échelle de l'Afrique dans le Précambrien de l'Ahaggar occidental. *Bull. Soc. géol. France*, **7**: 577-587.
- CABY, R.; ANDREOPOULOS-RENAUD, U. & LANCELLOT, J. R., (1985), Les phases tardives de l'orogénèse panafricaine dans l'Adrar des Iforas oriental (Mali): lithostratigraphie des formations molassiques et géochronologie U/Pb sur zircon de deux massifs intrusifs. *Precambrian Res.*, **28**: 187-199.
- CABY, R.; LIÉGEAIS, J. P.; DOSTAL, C.; DUPUY, C. & ANDREOPOULOS-RENAUD, U., (1986), The Tilemsi magmatic arc and the Pan-African suture zone in Northern Mali. *International Field Conf. on Proterozoic Geol. and Geochemistry, Colorado.* (Abstract).
- CAHEN, L. & SNELLING, N. J., (1984), *The geochronology of Africa.* Oxford University Press, Oxford.
- CORDANI, U. G. & IYER, S. S., (1979), Geochronological investigation on the Precambrian granulitic terrain of Bahia, Brazil. *Precambrian Res.*, **9**: 255-274.
- DEBON, F. & LE FORT, P., (1988), A cationic classification of common plutonic rocks and their magmatic associations: principles, method, applications. *Bull. Mineral.*, **111**: 493-510.
- DUCROT, J.; LA BOISSE, H.; DE RENAUD, U. & LANCELLOT, J. R., (1979), Synthèse géochronologique sur la succession des événements magmatiques Pan-Africains au Maroc, dans l'Adrar des Iforas et dans l'Est Hoggar. *10th Coll. Afr. Geol.*, Montpellier, avril 1979: p. 40.
- GUIRAUD, R. & ALIDOU, S., (1981), La faille de Kandi (Bénin), témoin du rejeu fini-crétacé d'un accident majeur à l'échelle de la plaque africaine. *C.R. Acad. Sci. Paris*, **293**: 779-782.
- HARRIS, N. B. W.; PEARCE, J. A. & TINDLE, A. G., (1986), Geochemical characteristics of collision-zone magmatism. In: *Collision Tectonics* (Coward M.P. & Ries A.C., eds.). *Geol. Soc. Spec. Pub.*, **19**: 67-81.
- KENNEDY, W. Q., (1964), The structural differentiation of Africa in the Pan-African ( $\pm$  500 m.y.) tectonic episode. *Res. Ist. Afr. Geol.*, Univ. Leeds, 8th Ann. Rep.: 48-49.
- LA ROCHE, H. DE; LETERRIER, J.; GRANCLAUDE, P. & MARCHAL, M., (1980), A classification of volcanic and plutonic rocks using R<sub>1</sub>R<sub>2</sub> diagram and major element analyses. Its relationships with current nomenclature. *Chem. Geol.*, **29**: 183-210.
- LIÉGEAIS, J. P. & BLACK, R., (1984), Pétrographie et géochronologie Rb-Sr de la transition calco-alkaline-alkaline fini-Pan-Africaine dans l'Adrar des Iforas (Mali): accretion crustale au Précambrien supérieur. In: *"African Geology", volume in honour of L. Cahen* (Klerks, J. & Michot, J., eds.): 115-145. Musée Royal de l'Afrique centrale, Tervuren.

- McCURRY, P., (1973), Geology of degree sheet 21 Zaria, Nigeria. *Overseas Geol. Min. Res.*, **45**, HMSO: 45 p.
- MCMURRY, J.; LONG, L. & SIAL, A. N., (1987), Petrology and isotopic systematics of magma mushes: some porphyritic granitoids of Northeastern Brazil. *Rev. Bras. Geociências*, **17**: 473-480.
- NOGUEIRA NETO, J. A.; TORQUATO, J. R. S.; ARTHAUD, M. H. & MACAMBIRA, M. J. B., (1989), Reavaliação e novos dados geocronológicos do Maciço Mediano de Granja (CE). *Atas do 13<sup>a</sup> Simpósio de Geologia do Nordeste*, Fortaleza, 1989: pp. 181-182.
- PATERSON, S. R.; VERNON, R. H. & TOBISCH, O. T., (1989), A review of criteria for the identification of magmatic and tectonic foliations in granitoids. *J. Struct. Geol.*, **11**: 349-363.
- STEIGER, R. H. & JÄGER, E., (1977), Subcommittee on Geochronology: convention on the use of decay constants in geo- and cosmochronology. *Earth Planet. Sci. Lett.*, **36**: 359-362.
- TUBOSUM, I. A.; LANCELOT, J. R.; RAHAMAN, M. A. & OCANIGER, O., (1984), U-Pb Pan-African ages of two charnockite-granite associations from Southwestern Nigeria. *Contrib. Mineral. Petrol.*, **88**: 188-195.
- VACHETTE, M., (1975), Age pan-africain des granites de Sinendé, Savé et Fita (Dahomey). *C.R. Acad. Sci. Paris*, **281**: 1793-1795.
- VAN BREEMEN, O.; PIDGEON, R. T. & BOWDEN, P., (1977), Age and isotopic studies of some pan-African granites from north-central Nigeria. *Precambrian Res.*, **4**: 307-319.
- VIALETTE, Y. & VITEL, G., (1979), Geochronological data on the Amsinassene-Tefedest block (central Hoggar, Algerian Sahara) and evidence for its polycyclic evolution. *Precambrian Res.*, **9**: 241-254.
- VITEL, G., (1975), Mylonitisation, tectonique cassante et linéamentaire du Hoggar Central; leurs rapports avec les granites d'âge pharusien. *Rev. Géogr. Phys. Géol. Dyn.*, **17**: 413-426.
- WILLIAMSON, J. H., (1968), Least-square fitting of a straight line. *Can. J. Phys.*, **46**: 1845-1847.